BrGDGT-based palaeothermometer in drylands: the necessity to constrain aridity and salinity as confounding factors to ensure the robustness of calibrations.

Lucas Dugerdil[1,2], Sébastien Joannin[1], Odile Peyron[1], Shafag Bayramova[3], Xiaozhong Huang[4,5], Fahu Chen[4,6,7], Dilfuza Egamberdieva[8,9], Jakhongir Alimov[10,11], Bazartseren Boldgiv[12], Amy Cromartie[13,1], Juzhi Hou[6,7], Lilit Sahakyan[14], Khachatur Meliksetian[14], Salomé Ansanay-Alex[2], Rafig Safarov[15], Imran Muradi[15], Shabnam Isayeva[16], Shehla Mirzayeva[16], Elshan Abdullayev[17,18], Sayyara Ibadullayeva[16], Parvana Garakhani[16], and Guillemette Ménot[2]

[1]ISEM, Univ Montpellier, CNRS, IRD, Montpellier, France
[2]ENS Lyon, UCBL, CNRS, UMR 5276 LGL-TPE, Lyon, France
[3]Institute of Geology and Geophysics, Department of modern geodynamics and space geodesy, Azerbaijan
[4]Key Laboratory of Western China's Environmental Systems (Ministry of Education), College of Earth and Environmental Sciences, Lanzhou University, Lanzhou, China
[5]Yunnan Key Laboratory of Plateau Geographical Processes and Environmental Changes, Faculty of Geography, Yunnan Normal University, Kunming 650500, China
[6]Alpine Paleoecology and Human Adaptation Group, State Key Laboratory of Tibetan Plateau Earth System, Resources and Environment, Institute of Tibetan Plateau Research, Chinese Academy of Sciences, Beijing, China
[7]College of Resources and Environment, University of Chinese Academy of Sciences, Beijing, China
[8]Institute of Fundamental and Applied Research, National Research Univ. (TIIAME), Tashkent 100000, Uzbekistan
[9]Leibniz Centre for Agricultural Landscape Research (ZALF), 15374 Müncheberg, Germany
[10]International Agriculture University, Kibray district, 100164, Tashkent, Uzbekistan
[11]Faculty of Biology, National University of Uzbekistan, 100174, Tashkent, Uzbekistan
[12]Ecology Group, Department of Biology, School of Arts and Sciences, National University of Mongolia, Ulaanbaatar 14201, Mongolia
[13]Université Côte d'Azur, CNRS, CEPAM, UMR 7264, 06300, Nice, France
[14]National Academy of Sciences, Institute of Geological Sciences of Armenia, ave. M. Baghramyan 24a, Yerevan 0019, Armenia
[15]Institute of Geology and Geophysics, Science and Education Ministry of Azerbaijan Republic, AZ1073, Baku, Azerbaijan
[16]Institute of Botany, Azerbaijan National Academy of Sciences, Baku, Azerbaijan
[17]Institute of Geography and Geology, University of Greifswald, Friedrich-Ludwig-Jahn Strasse 17A, D-17487 Greifswald, Germany
[18]Department of Life Sciences, Khazar University, 41 Mahsati Str., AZ1096 Baku, Azerbaijan

Correspondence: Lucas Dugerdil (lucas.dugerdil@ens-lyon.fr) and Guillemette Ménot (guillemette.menot@ens-lyon.fr)

Abstract. Past temperature reconstructions offer valuable insights into the impact of climate change on the global climate-human-vegetation system. Branched glycerol dialkyl glycerol tetraethers (brGDGTs) are recognized as effective temperature proxies, particularly in lakes and peatlands, where they are well preserved. However, their reliability as palaeothermometers can be compromised by factors beyond air temperature, especially in drylands. This study introduces the Arid Central Asian (ACA) brGDGT surface Data Base, a regional dataset consisting of 162 new surface samples from the drylands of ACA, in addition to 599 previously published samples. The distribution of brGDGTs in relation to climate and environmental variables

was analysed to explore their potential as reliable temperature proxies, mainly focusing on brGDGTs methylation (MBT), cyclisation (CBT), and isomer (IR) indices. The brGDGT-based palaeothermometer is a promising tool for understanding past climates, but our comparison between an ACA-centred database and a worldwide continental surface sample database reveals several challenges. Drylands exhibit extreme climate and soil/lacustrine properties, amplifying the impact of confounding factors on brGDGT-based relationships with mean annual air temperature. Salinity emerges as the dominant factor influencing brGDGT variance, followed by sample type, salinity, pH, and aridity, all of which contribute significantly. These factors interact in complex ways, with the salinity effect varying between soil and lacustrine deposits. For sample physicochemical conditions, the $\mathrm{IR}'_{6+7\mathrm{Me}}$ index is best for salinity, and $\mathrm{IR}_{6\mathrm{Me}}$ is most suitable for pH reconstruction. Despite this, the $\mathrm{MBT}'_{5\mathrm{Me}}$-temperature relationship is limited in ACA, particularly for lacustrine samples, and $\mathrm{MBT}'_{6\mathrm{Me}}$ does not offer a better solution under hyper- to semi-arid conditions. Sub-calibrating models for specific environmental conditions such as salinity and aridity improves the accuracy of temperature reconstructions. Furthermore, the difference between $\mathrm{MBT}'_{5\mathrm{Me}}$ and $\mathrm{MBT}'_{6\mathrm{Me}}$ provides a promising proxy to assess aridity. Although the brGDGT signal in drylands is influenced by multiple confounding factors, it remains a valuable tool for understanding past climate and environmental conditions, especially when accounting for the complex interactions between these factors based on each study's unique physicochemical and bioclimatic context. Further research, incorporating a broader range of surface samples alongside comprehensive soil and climate data, holds the potential to enhance the accuracy of brGDGT-based climate reconstructions.

1 Supplementary Figures

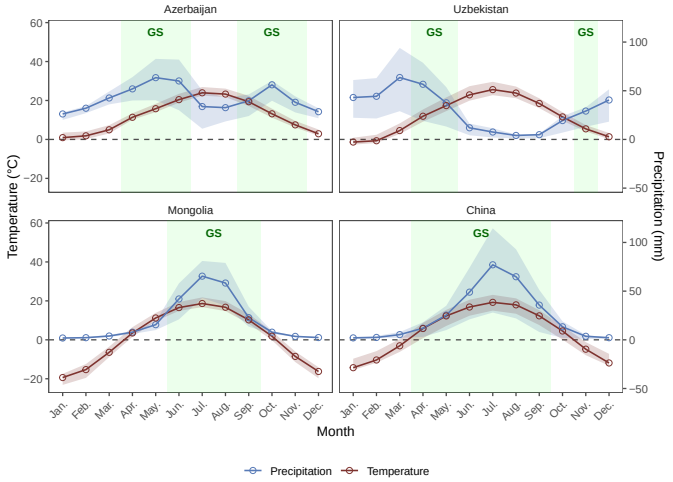

Figure S.1. Ombrothermic diagrams for four regions of the ACA: Azerbaijan, Uzbekistan Mongolia and China. The climate parameters were extracted from `worldclim2.1` (Fick and Hijmans, 2017) at the sample location of the ACADB sites. The estimated Growth Season (GS) was roughly determined with T > 5 °C and $P > 2 \times T$.

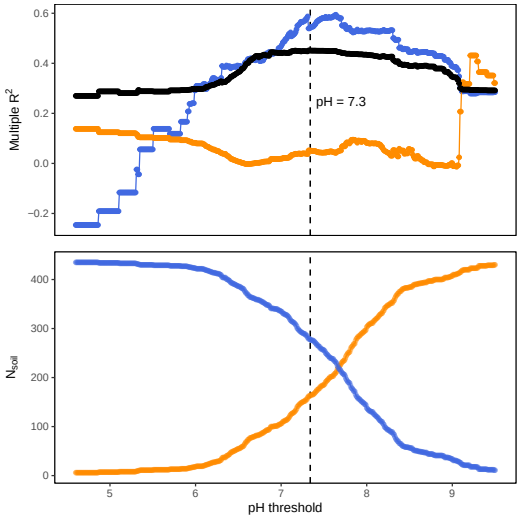

Figure S.2. Graphical determination of the more efficient pH threshold affecting the bimodal distribution of CBT' against pH for soil samples. The pH threshold values were implemented from 4 to 11 for each 0.01 step. The maximum multiple R^2 is found for pH = 7.3. The lower panel shows the number of samples for each cluster. In blue are given the results for the *acidic* soils (i.e., the samples below the threshold), in orange the *alkaline* soils (above the threshold), and in black the overall multiple R^2.

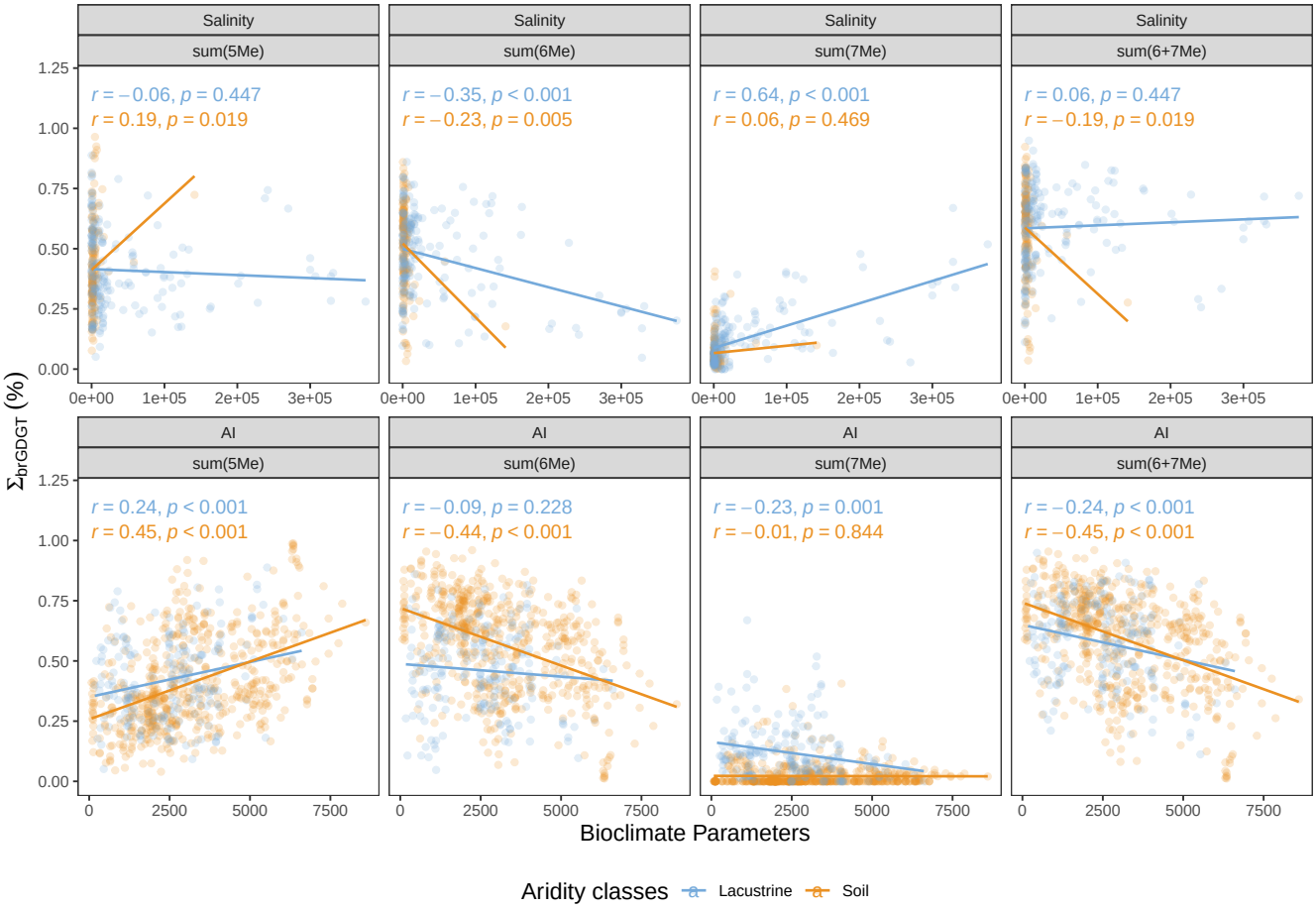

Figure S.3. Effect of the salinity and the aridity on the sum of 5-, 6-, 7-methyl and 6+7-methyl FAs for soil and lacustrine samples.

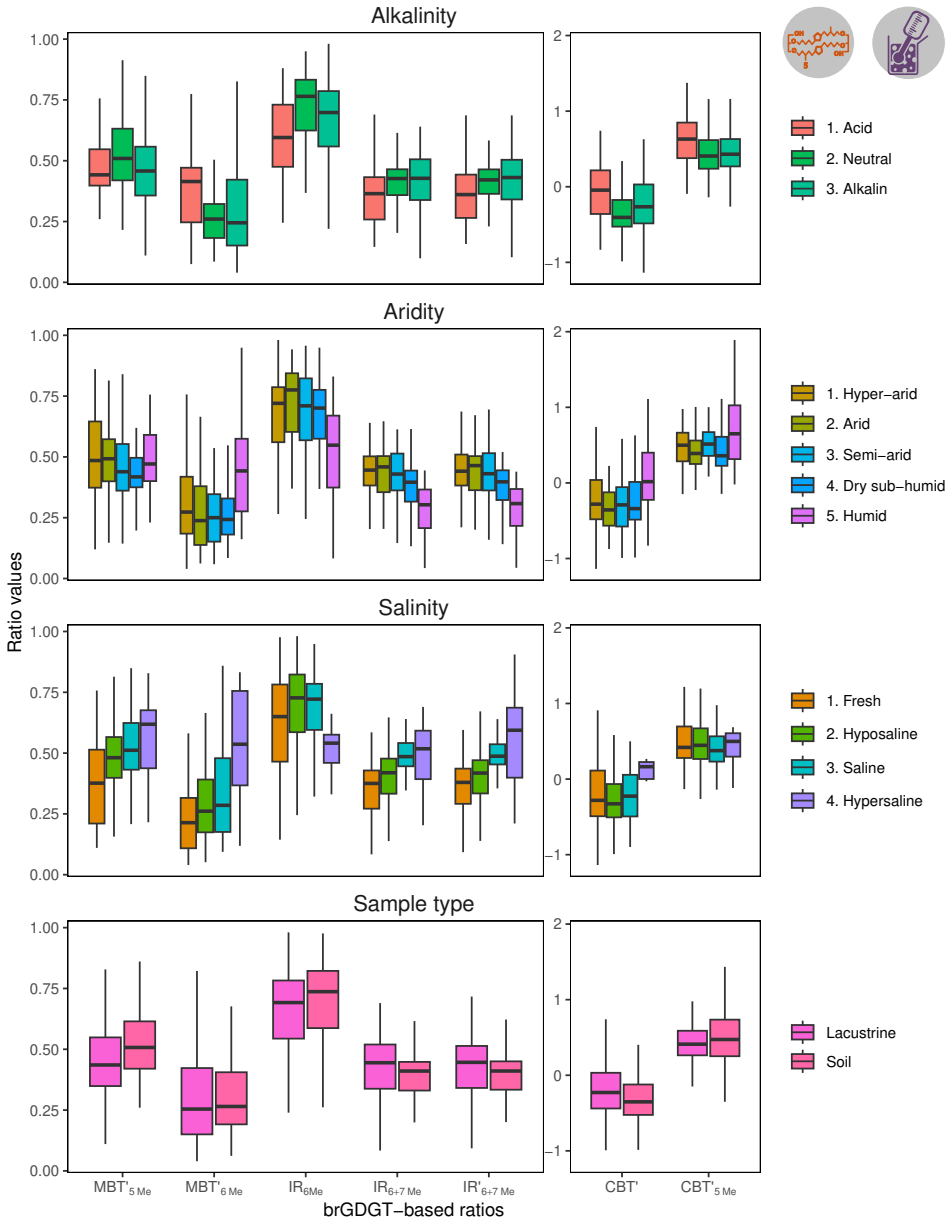

Figure S.4. Boxplot for the main brGDGT-based ratios presented in this study clustered by the four grouping factors (i.e., alkalinity, aridity, salinity, and sample type). This figure is associated with the MANOVA and ANOVA results of Table 3.

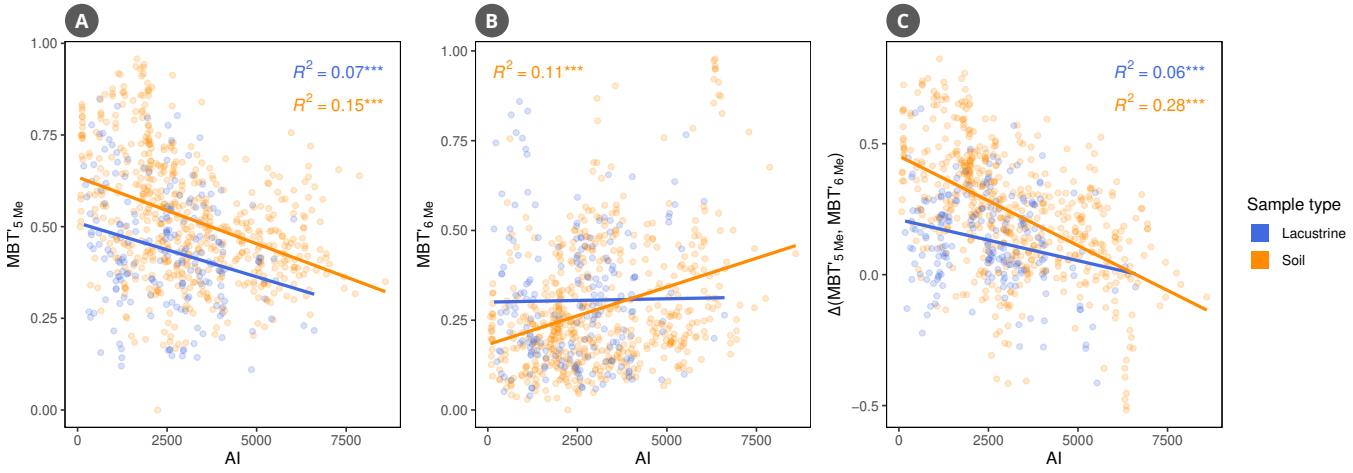

Figure S.5. Relationships between the Aridity Index (AI) and Methylation indices, i.e. $\mathrm{MBT'_{5Me}}$ (**A**), $\mathrm{MBT'_{6Me}}$ (**B**), and $\Delta(\mathrm{MBT'_{5Me}}, \mathrm{MBT'_{6Me}})$ (**C**) linear relationships with AI. The regressions were tested for soil (orange) and lacustrine (blue) samples. Solely, the R^2 for significant regression (p-value < 0.001) were displayed.

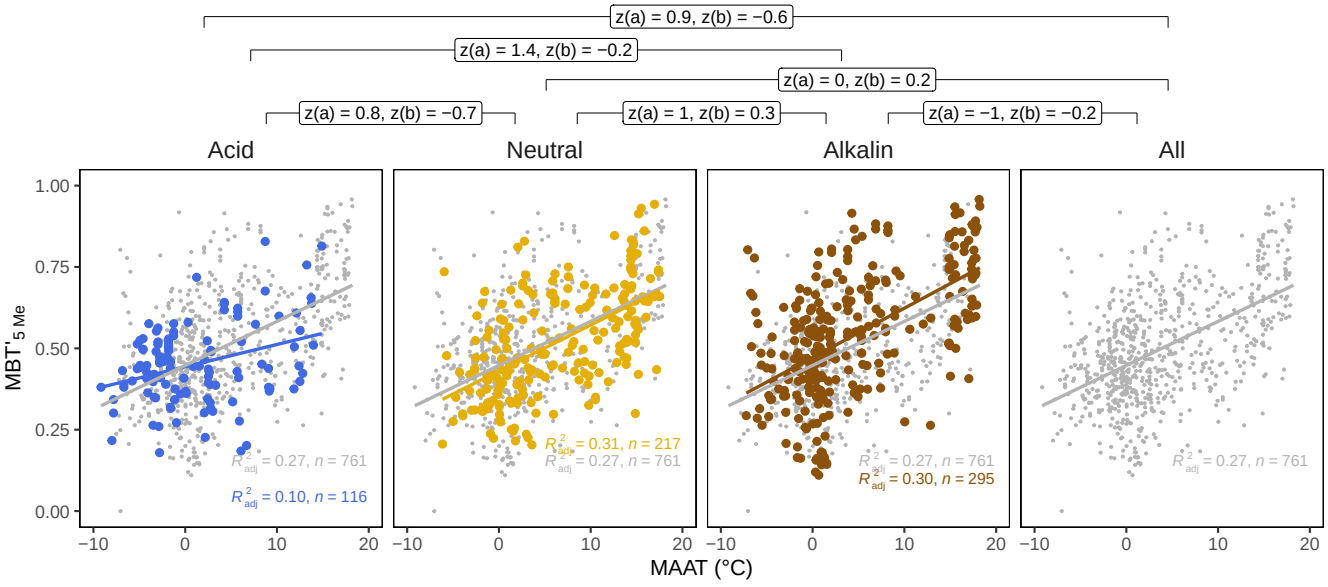

Figure S.6. Effect of the alkalinity (i.e., the pH of each surface sample) on the linear relation between temperature (here MAAT) and the $\mathrm{MBT'_{5Me}}$. Based on the alkalinity classes (i.e., acid, neutral, and alkaline), different temperature calibration $\mathrm{MBT'_{5Me}}$-based are proposed following MAAT = a $\times$ $\mathrm{MBT'_{5Me}}$ + b. Using the z-statistic with its p-value (Clogg et al., 1995), the significance of the difference between the slopes (a) of the linear regression is evaluated. Similarly, the z-statistic was used for the intercept (b) differences. For the p-values we have *** for p $\leq$ 0.01, ** for p $\leq$ 0.05 and * for p $\leq$ 0.1.

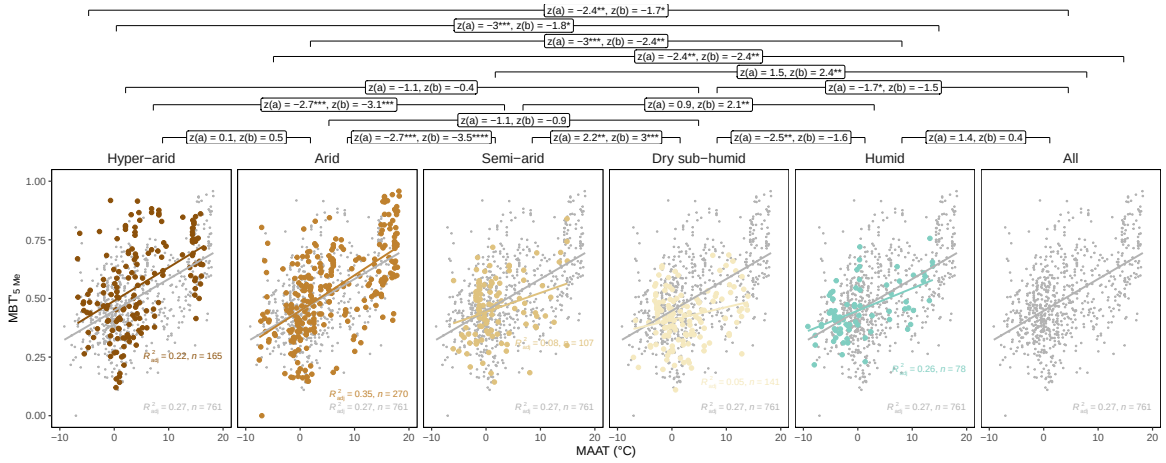

Figure S.7. Effect of the aridity (i.e. the AI of each surface sample) on the linear relation between temperature (here MAAT) and the $\mathrm{MBT}'_{5\mathrm{Me}}$. Based on the aridity classes (i.e., hyper-arid, arid, semi-arid, dry sub-humid, and humid), different temperature calibration $\mathrm{MBT}'_{5\mathrm{Me}}$-based are proposed following MAAT = a $\times$ $\mathrm{MBT}'_{5\mathrm{Me}}$ + b. Using the z-statistic with its p-value (Clogg et al., 1995), the significance of the difference between the slopes (a) of the linear regression is evaluated. Similarly, the z-statistic was used for the intercept (b) differences. For the p-values we have *** for p $\leq$ 0.01, ** for p $\leq$ 0.05, and * for p $\leq$ 0.1.

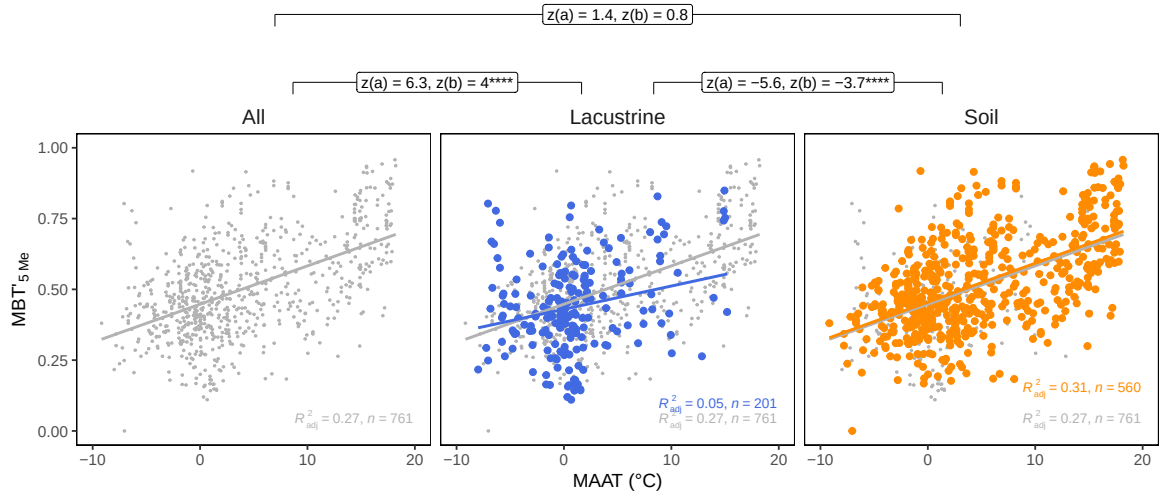

Figure S.8. Effect of the sample type on the linear relation between temperature (here MAAT) and the $\mathrm{MBT}'_{5\mathrm{Me}}$. Based on the sample types (i.e., soil or lacustrine), different temperature calibration $\mathrm{MBT}'_{5\mathrm{Me}}$-based are proposed following MAAT = a $\times$ $\mathrm{MBT}'_{5\mathrm{Me}}$ + b. Using the z-statistic with its p-value (Clogg et al., 1995), the significance of the difference between the slopes (a) of the linear regression is evaluated. Similarly, the z-statistic was used for the intercept (b) differences. For the p-values we have *** for p $\leq$ 0.01, ** for p $\leq$ 0.05, and * for p $\leq$ 0.1.

2 Supplementary Tables

Table S.1: Geographical and biological presentation of the new surface sites of the ACADB presented in this study.

Sites	Longitude	Latitude	Altitude	Date	Country	Sample type	Ecosystem	pH	Salinity
MAZT1C02	46.99	40.99	109	2021	Azerbaijan	Lacustrine	Halophytic desert	8.11	124839.00
MAZT1C06	45.77	41.19	550	2021	Azerbaijan	Lacustrine	Shrub desert	8.53	2016.95
MAZT1M01	46.99	40.99	112	2021	Azerbaijan	Soil	Halophytic desert	8.37	2249.00
MAZT1M03	47.00	41.01	138	2021	Azerbaijan	Soil	Halophytic desert	8.41	1001.00
MAZT1M04	45.77	41.18	597	2021	Azerbaijan	Soil	Shrub desert	5.82	2314.00
MAZT1M07	45.74	41.06	246	2021	Azerbaijan	Soil	Shrub desert	7.18	3185.00
MAZT1M08	45.79	41.01	288	2021	Azerbaijan	Soil	Shrub desert	7.34	2522.00
MAZT1M09	47.78	40.71	222	2022	Azerbaijan	Soil	Thermophilous woodland	7.61	2008.50
MAZT1M10	46.91	41.21	391	2022	Azerbaijan	Soil	Thermophilous woodland	7.09	1111.50
MAZT1M11	46.05	40.70	668	2022	Azerbaijan	Soil	Thermophilous woodland	6.81	2405.00
MAZT1S05	45.77	41.19	552	2021	Azerbaijan	Soil	Shrub desert	7.67	1612.00
MAZT2C02	46.26	40.37	1722	2021	Azerbaijan	Lacustrine	Deciduous forest	6.81	507.00
MAZT2C05	46.59	40.64	273	2021	Azerbaijan	Lacustrine	Halophytic desert	7.57	3302.00
MAZT2M01	46.28	40.40	1412	2021	Azerbaijan	Soil	Deciduous forest	6.79	1469.00
MAZT2M03	46.27	40.37	1820	2021	Azerbaijan	Soil	Deciduous forest	6.49	1313.00
MAZT2M04	46.36	40.46	1232	2021	Azerbaijan	Soil	Deciduous forest	7.50	1274.00
MAZT2M06	46.96	40.55	96	2021	Azerbaijan	Soil	Shrub desert	7.96	1092.00
MAZT2M07	45.75	40.54	1660	2022	Azerbaijan	Soil	Grasslands	7.11	1229.80
MAZT3C01	47.76	40.11	-10	2021	Azerbaijan	Lacustrine	Halophytic desert	7.96	4399.20
MAZT3C03	47.61	39.89	15	2021	Azerbaijan	Lacustrine	Halophytic desert	8.98	90530.05
MAZT3M04	47.61	39.90	15	2021	Azerbaijan	Soil	Halophytic desert	7.45	877.50
MAZT3M06	47.28	39.97	86	2022	Azerbaijan	Soil	Halophytic desert	7.26	2620.15
MAZT3M07	47.99	39.88	-2	2022	Azerbaijan	Soil	Halophytic desert	9.11	4134.00
MAZT3S02	47.59	40.09	-4	2021	Azerbaijan	Soil	Halophytic desert	8.90	16705.00
MAZT3S05	47.60	39.90	12	2021	Azerbaijan	Soil	Halophytic desert	9.05	23029.50
MAZT4M01	48.88	40.70	846	2022	Azerbaijan	Soil	Steppe	7.80	942.50
MAZT4M02	48.57	40.85	1485	2022	Azerbaijan	Soil	Steppe	7.63	926.90
MAZT4M03	47.97	40.87	522	2022	Azerbaijan	Soil	Deciduous forest	7.74	1072.50
MAZT4M04	47.90	41.05	1956	2022	Azerbaijan	Soil	Deciduous forest	8.21	1638.00
MAZT4M05	47.81	41.09	1732	2022	Azerbaijan	Soil	Deciduous forest	7.83	390.00
MAZT4M06	47.43	41.06	517	2022	Azerbaijan	Soil	Thermophilous woodland	7.39	1519.05
MAZT4M07	47.13	41.30	898	2022	Azerbaijan	Soil	Deciduous forest	6.18	1318.20
MAZT4M08	46.56	41.70	626	2022	Azerbaijan	Soil	Deciduous forest	8.58	2496.00
MAZT4M09	46.47	41.63	242	2022	Azerbaijan	Soil	Deciduous forest	6.86	1462.50
MAZT4M10	46.77	41.58	643	2022	Azerbaijan	Soil	Deciduous forest	6.57	1092.65
MAZT4M11	46.79	41.31	204	2022	Azerbaijan	Soil	Deciduous forest	6.48	741.00
MAZT4M12	48.14	41.18	2150	2022	Azerbaijan	Soil	Steppe	6.96	487.50
MAZT4M13	48.44	41.26	900	2022	Azerbaijan	Soil	Deciduous forest	7.39	2262.00
MAZT4M14	48.71	40.81	1382	2022	Azerbaijan	Soil	Steppe	7.93	936.00
MAZT5M03	49.15	39.42	-28	2022	Azerbaijan	Soil	Shrub desert	7.51	1209.00
MAZT5M04	48.91	39.88	-22	2022	Azerbaijan	Soil	Halophytic desert	7.96	955.50
MAZT5M05	48.95	40.08	58	2022	Azerbaijan	Soil	Shrub desert	7.51	682.50
MAZT5S01	48.48	39.27	19	2022	Azerbaijan	Soil	Shrub desert	7.56	799.50
MAZT5S02	49.21	39.28	-28	2022	Azerbaijan	Soil	Halophytic desert	7.75	14872.65
MAZT5S06	49.34	40.90	-24	2022	Azerbaijan	Soil	Halophytic desert	7.28	7936.50
MAZT5S07	49.22	40.57	493	2022	Azerbaijan	Soil	Shrub desert	4.17	4368.00
MAZT6M01	48.66	38.86	85	2022	Azerbaijan	Soil	Hyrcanian forest	6.11	546.00
MAZT6M02	48.74	38.77	84	2022	Azerbaijan	Soil	Hyrcanian forest	6.35	390.00
MCNT1M01	100.54	36.32	3012	2016	China, Qinghai	Soil	*Achnatherum splendens* steppe	5.98	2262.00
MCNT1M04	100.59	36.41	3545	2016	China, Qinghai	Soil	*Kobresia pygmaea* alpine meadow	7.17	1917.50
MCNT1M05	100.47	36.54	3736	2016	China, Qinghai	Soil	*Stipa breviflora* desert steppe	7.01	3861.00
MCNT1M06	100.47	36.55	3519	2016	China, Qinghai	Soil	*Stipa breviflora* desert steppe	7.21	5660.20
MCNT1M07	100.47	36.55	3519	2016	China, Qinghai	Soil	*Stipa breviflora* desert steppe	7.76	1622.40
MCNT1M09	100.72	36.54	3205	2016	China, Qinghai	Soil	*Achnatherum splendens* steppe	7.75	1501.50
MCNT1M11	100.79	36.81	3240	2016	China, Qinghai	Soil	*Achnatherum splendens* steppe	7.91	745.55
MCNT1M13	100.62	37.09	3329	2016	China, Qinghai	Soil	*Kobresia pygmaea* alpine meadow	7.89	1625.65
MCNT1M14	100.64	37.25	3393	2016	China, Qinghai	Soil	*Stipa purpurea* alpine steppe		
MCNT1M15	100.68	37.33	3511	2016	China, Qinghai	Soil	*Dasiphora fruticosa* scrub	7.52	4395.30
MCNT1M16	100.75	37.32	3613	2016	China, Qinghai	Soil	*Dasiphora fruticosa* scrub		
MCNT1M17	100.80	37.33	3724	2016	China, Qinghai	Soil	*Dasiphora fruticosa* scrub	7.81	4894.50
MCNT1M18	100.80	37.36	3811	2016	China, Qinghai	Soil	*Dasiphora fruticosa* scrub	7.53	5005.00
MCNT1M19	100.82	37.38	4038	2016	China, Qinghai	Soil	*Saussurea* spp. sparse vegetation	7.45	2496.00
MCNT1M20	100.82	37.39	4038	2016	China, Qinghai	Soil	*Saussurea* spp. sparse vegetation		
MCNT1M21	100.82	37.39	4038	2016	China, Qinghai	Soil	*Saussurea* spp. sparse vegetation		
MCNT1M22	101.10	37.48	4012	2016	China, Qinghai	Soil	*Dasiphora fruticosa* scrub		

MCNT1M23	101.10	37.48	3936	2016	China, Qinghai	Soil	*Dasiphora fruticosa* scrub		
MCNT1M24	101.11	37.49	3936	2016	China, Qinghai	Soil	*Dasiphora fruticosa* scrub	4.41	9607.65
MCNT1M25	101.11	37.50	3814	2016	China, Qinghai	Soil	*Dasiphora fruticosa* scrub	5.34	5239.00
MCNT1M26	101.12	37.51	3670	2016	China, Qinghai	Soil	*Kobresia pygmaea* alpine meadow	6.40	3744.00
MCNT1M27	101.15	37.51	3541	2016	China, Qinghai	Soil	*Kobresia pygmaea* alpine meadow	6.00	4430.40
MCNT1M28	101.19	37.50	3326	2016	China, Qinghai	Soil	*Kobresia pygmaea* alpine meadow	6.15	9701.25
MCNT1M31	101.32	37.66	3322	2016	China, Qinghai	Soil	*Dasiphora fruticosa* scrub	7.10	8927.10
MCNT1M32	101.20	37.77	3418	2016	China, Qinghai	Soil	*Dasiphora fruticosa* scrub	6.87	5265.00
MCNT1M33	101.14	37.83	3671	2016	China, Qinghai	Soil	*Kobresia pygmaea* alpine meadow	7.64	5705.70
MCNT1M34	101.11	37.84	3758	2016	China, Qinghai	Soil	*Kobresia pygmaea* alpine meadow	6.82	4664.40
MCNT1M35	101.07	37.86	3590	2016	China, Qinghai	Soil	*Kobresia pygmaea* alpine meadow	6.55	9272.25
MCNT1M36	100.94	38.16	3049	2016	China, Qinghai	Soil	*Salix gilashanica* scrub	6.96	7616.70
MCNT1M37	100.93	38.19	3005	2016	China, Qinghai	Soil	*Salix gilashanica* scrub	7.18	6674.20
MCNT1M38	100.93	38.25	2780	2016	China, Qinghai	Soil	*Kobresia* spp., *Carex* spp. alpine meadow	8.20	1131.00
MCNT1M39	100.94	38.30	2646	2016	China, Qinghai	Soil	*Stipa breviflora, S.bungeana* steppe	7.40	4290.00
MCNT1M40	100.91	38.37	2492	2016	China, Qinghai	Soil	*Stipa breviflora, S.bungeana* steppe	8.50	1657.50
MCNT1M41	101.04	38.39	2420	2016	China, Qinghai	Soil	*Stipa breviflora, S.bungeana* steppe	7.75	12421.50
MCNT1M42	101.09	38.46	2265	2016	China, Qinghai	Soil	*Stipa breviflora, S.bungeana* steppe	7.94	1565.20
MCNT1M47	101.11	38.87	2276	2016	China, Qinghai	Soil	Dwarf needlegrass desert steppe	8.79	1039.35
MCNT1S02	100.59	36.37	3148	2016	China, Qinghai	Soil	*Kobresia pygmaea* alpine meadow	7.68	273.00
MCNT1S03	100.59	36.39	3357	2016	China, Qinghai	Soil	*Kobresia pygmaea* alpine meadow	7.54	399.75
MCNT1S10	100.79	36.71	3235	2016	China, Qinghai	Soil	*Artemisia arenaria* desert	8.97	104.00
MCNT1S12	100.58	37.04	3198	2016	China, Qinghai	Soil	*Achnatherum splendens* steppe	9.13	5038.80
MCNT1S29	101.23	37.52	3127	2016	China, Qinghai	Soil	*Dasiphora fruticosa* scrub	9.10	1296.75
MCNT1S30	101.25	37.62	3161	2016	China, Qinghai	Soil	*Dasiphora fruticosa* scrub	8.53	1344.20
MCNT1S45	101.09	38.84	1903	2016	China, Qinghai	Soil	Dwarf needlegrass desert steppe	9.30	390.00
MCNT1S48	101.09	38.88	2235	2016	China, Qinghai	Soil	*Stipa breviflora, S.bungeana* steppe	9.48	358.80
MCNT1S49	101.11	38.90	2057	2016	China, Qinghai	Soil	*Stipa breviflora, S.bungeana* steppe	9.04	2639.00
MCNT1S50	101.18	38.96	1885	2016	China, Qinghai	Soil	Dwarf needlegrass desert steppe	9.56	1394.90
MCNT1S53	101.39	39.13	1499	2016	China, Qinghai	Soil	*Reaumuria soongorica* desert	10.35	304.20
MCNT1S54	101.50	39.19	1435	2016	China, Qinghai	Soil	*Reaumuria soongorica* desert	9.91	764.40
MTAT1M01	71.52	38.86	2624	2021	Tajikistan	Soil	*Yailau* cryophilous open woodlands	7.24	666.90
MTAT1M02	71.60	38.81	2799	2021	Tajikistan	Soil	*Yailau* cryophilous open woodlands	6.76	702.00
MTAT1M03	71.69	38.76	3046	2021	Tajikistan	Soil	*Yailau* cryophilous open woodlands	6.82	382.20
MTAT1M06	71.88	38.51	3984	2021	Tajikistan	Soil	*Yailau* mesic grasslands	5.92	2068.30
MTAT1M07	71.88	38.45	3164	2021	Tajikistan	Soil	*Yailau* cryophilous open woodlands	7.18	2359.50
MTAT1M08	71.83	38.38	2472	2021	Tajikistan	Soil	*Yailau* cryophilous open woodlands	6.95	2223.00
MTAT1M09	71.79	38.37	2397	2021	Tajikistan	Soil	*Yailau* cryophilous open woodlands	7.41	838.50
MTAT2M01	68.23	38.65	1220	2022	Tajikistan	Soil	*Tau* xeric shrublands	6.56	6006.00
MTAT2M02	69.98	38.11	1251	2022	Tajikistan	Soil	*Tau* xeric shrublands	7.41	915.20
MTAT2M03	69.97	38.86	1150	2022	Tajikistan	Soil	*Tau* xeric shrublands	7.01	1774.50
MTAT2M04	70.03	38.86	1198	2022	Tajikistan	Soil	*Tau* xeric shrublands	7.23	1150.50
MTAT2M05	68.52	39.21	2052	2022	Tajikistan	Soil	*Tau* steppes	6.91	4712.50
MUZT1C04	69.84	41.40	1418	2021	Uzbekistan	Lacustrine	*Tau* xeric shrublands	7.83	2574.00
MUZT1C05	69.85	41.42	1272	2021	Uzbekistan	Lacustrine	*Tau* open woodlands	8.19	6006.00
MUZT1M01	69.84	41.40	1420	2021	Uzbekistan	Soil	*Tau* open woodlands	7.86	546.00
MUZT1M06	70.14	41.15	1646	2022	Uzbekistan	Soil	*Tau* open woodlands	7.06	1433.25
MUZT1S02	69.85	41.42	1291	2021	Uzbekistan	Soil	*Tau* steppes	8.00	741.00
MUZT1S03	69.85	41.42	1284	2021	Uzbekistan	Soil	*Tau* steppes	7.89	2676.70
MUZT2C01	66.88	39.33	1796	2021	Uzbekistan	Lacustrine	*Tau* steppes	6.66	897.00
MUZT2M02	66.88	39.33	1801	2021	Uzbekistan	Soil	*Tau* steppes	6.63	312.00
MUZT2M04	67.39	39.83	816	2022	Uzbekistan	Soil	*Adyr* steppes	7.04	1170.00
MUZT2M06	66.92	39.28	1424	2022	Uzbekistan	Soil	*Tau* xeric shrublands	7.76	1338.35
MUZT2M07	67.41	39.54	870	2022	Uzbekistan	Soil	*Tau* xeric shrublands	7.25	526.50
MUZT2M08	66.52	39.50	912	2022	Uzbekistan	Soil	*Tau* xeric shrublands	7.18	1158.30
MUZT2S03	66.88	39.35	1727	2021	Uzbekistan	Soil	*Tau* steppes	6.53	251.55
MUZT2S05	66.19	39.86	516	2022	Uzbekistan	Soil	*Adyr* pseudosteppes	7.80	507.00
MUZT3C02	66.70	38.13	1646	2021	Uzbekistan	Lacustrine	*Tau* open woodlands	8.18	1014.00
MUZT3C04	66.71	38.12	1847	2021	Uzbekistan	Lacustrine	*Tau* open woodlands	7.98	9165.00
MUZT3C19	66.73	38.08	1672	2023	Uzbekistan	Lacustrine	*Tau* open woodlands		
MUZT3M03	66.70	38.12	1740	2021	Uzbekistan	Soil	*Tau* open woodlands	7.71	624.00
MUZT3M05	67.76	38.62	1582	2021	Uzbekistan	Soil	*Tau* open woodlands	7.38	760.50
MUZT3M07	67.69	38.66	3038	2021	Uzbekistan	Soil	*Yailau* mesic grasslands	7.51	1384.50
MUZT3M08	67.66	38.64	3121	2021	Uzbekistan	Soil	*Yailau* mesic grasslands	7.45	841.75
MUZT3M09	66.91	38.21	1236	2022	Uzbekistan	Soil	*Adyr* steppes	7.22	1228.50
MUZT3M10	66.73	38.09	1709	2022	Uzbekistan	Soil	*Tau* open woodlands	7.11	2457.00
MUZT3M11	66.77	38.68	1308	2022	Uzbekistan	Soil	*Tau* xeric shrublands	6.73	5253.95
MUZT3M12	67.03	38.21	1077	2022	Uzbekistan	Soil	*Tau* xeric shrublands	7.31	663.00
MUZT3M13	66.73	37.61	786	2022	Uzbekistan	Soil	*Adyr* pseudosteppes	7.30	1228.50
MUZT3M14	66.76	37.77	958	2022	Uzbekistan	Soil	*Adyr* steppes	6.86	3178.50
MUZT3M15	66.74	37.63	664	2022	Uzbekistan	Soil	*Adyr* steppes	7.28	838.50
MUZT3M16	66.79	37.79	936	2022	Uzbekistan	Soil	*Adyr* steppes	7.74	2905.50
MUZT3M17	66.69	37.63	713	2022	Uzbekistan	Soil	*Adyr* steppes	7.47	897.00
MUZT3M18	66.70	37.78	1130	2022	Uzbekistan	Soil	*Tau* xeric shrublands	7.49	1774.50

MUZT3S06	67.71	38.65	2442	2021	Uzbekistan	Soil	*Yailau* cryophilous open woodlands	6.87	1625.00
MUZT4C02	64.22	39.64	200	2021	Uzbekistan	Lacustrine	*Chul* deserts	9.02	121649.45
MUZT4C04	64.24	39.63	208	2021	Uzbekistan	Lacustrine	*Chul* deserts	8.89	122995.60
MUZT4M05	64.91	40.09	292	2022	Uzbekistan	Soil	*Adyr* pseudosteppes	7.43	526.50
MUZT4M09	64.31	39.11	272	2022	Uzbekistan	Soil	*Chul* deserts	7.54	604.50
MUZT4S01	65.10	39.33	280	2021	Uzbekistan	Soil	*Chul* deserts	7.28	11778.00
MUZT4S03	64.22	39.64	204	2021	Uzbekistan	Soil	*Chul* deserts	8.48	141255.40
MUZT4S06	64.86	38.96	272	2022	Uzbekistan	Soil	*Chul* deserts	7.91	273.00
MUZT4S07	65.05	39.06	288	2022	Uzbekistan	Soil	*Chul* deserts	8.24	1111.50
MUZT5C02	63.21	41.77	53	2021	Uzbekistan	Soil	*Chul* deserts	8.33	57943.60
MUZT5M03	63.85	42.52	366	2022	Uzbekistan	Soil	*Chul* deserts	7.55	916.50
MUZT5M04	64.15	42.93	257	2022	Uzbekistan	Soil	*Chul* deserts	7.75	320.45
MUZT5M05	62.82	42.31	97	2022	Uzbekistan	Soil	*Chul* deserts	7.80	487.50
MUZT5M06	63.43	42.20	194	2022	Uzbekistan	Soil	*Chul* deserts	7.54	604.50
MUZT5S08	63.27	40.27	180	2022	Uzbekistan	Soil	*Chul* deserts	8.34	390.00
MUZT6C02	66.59	40.55	1644	2021	Uzbekistan	Lacustrine	*Tau* steppes	7.75	3336.45
MUZT6M03	66.63	40.57	1166	2021	Uzbekistan	Soil	*Tau* xeric shrublands	7.66	955.50
MUZT6M04	66.66	40.58	836	2021	Uzbekistan	Soil	*Tau* xeric shrublands	7.92	2145.00
MUZT6S01	66.62	40.57	1460	2021	Uzbekistan	Soil	*Tau* steppes	7.62	487.50
MUZT7C01	58.99	44.86	38	2023	Uzbekistan	Lacustrine	*Chul* deserts	9.11	237994.90
MUZT7C02	58.49	44.80	29	2023	Uzbekistan	Lacustrine	*Chul* deserts	8.25	77231.70
MUZT7C03	58.65	44.73	31	2023	Uzbekistan	Lacustrine	*Chul* deserts	8.82	36718.50
MUZT7C04	58.73	44.73	29	2023	Uzbekistan	Lacustrine	*Chul* deserts	8.72	241833.80

Table S.2: List of the different references compiled mainly from Raberg et al. (2022) plus other studies; to build the ACADB and the WDB used in this study.

DB	Reference	N sites	Study area	Citation
ACA	Chen et al. (2021)	53	Tajikistan	Chen, C., Bai, Y., Fang, X., Zhuang, G., Khodzhiev, A., Bai, X., and Murodov, A.: Evaluating the Potential of Soil Bacterial Tetraether Proxies in Westerlies Dominating Western Pamirs, Tajikistan and Implications for Paleoenvironmental Reconstructions, Chemical Geology, 559, 119 908, https://doi.org/10.1016/j.chemgeo.2020.119908, 2021
ACA	Dang et al. (2018)	10	China	Dang, X., Ding, W., Yang, H., Pancost, R. D., Naafs, B. D. A., Xue, J., Lin, X., Lu, J., and Xie, S.: Different Temperature Dependence of the Bacterial brGDGT Isomers in 35 Chinese Lake Sediments Compared to That in Soils, Organic Geochemistry, 119, 72–79, https://doi.org/10/gdfs3x, 2018
ACA	De Jonge et al. (2015a), Khodzher et al. (2017)	8	Russia, Baikal	De Jonge, C., Stadnitskaia, A., Fedotov, A., and Sinninghe Damsté, J. S.: Impact of Riverine Suspended Particulate Matter on the Branched Glycerol Dialkyl Glycerol Tetraether Composition of Lakes: The Outflow of the Selenga River in Lake Baikal (Russia), Organic Geochemistry, 83–84, 241–252, https://doi.org/10.1016/j.orggeochem.2015.04.004, 2015, Khodzher, T. V., Domysheva, V. M., Sorokovikova, L. M., Sakirko, M. V., and Tomberg, I. V.: Current Chemical Composition of Lake Baikal Water, Inland Waters, 7, 250–258, https://doi.org/10.1080/20442041.2017.1329982, 2017
ACA	Dearing Crampton-Flood et al. (2020)	15	Global BayMBT Soils	Dearing Crampton-Flood, E., Tierney, J. E., Peterse, F., Kirkels, F. M. S. A., and Sinninghe Damsté, J. S.: BayMBT: A Bayesian Calibration Model for Branched Glycerol Dialkyl Glycerol Tetraethers in Soils and Peats, Geochimica et Cosmochimica Acta, 268, 142–159, https://doi.org/10/gg9758, 2020
ACA	Duan et al. (2020)	18	China, Tian Shan	Duan, Y., Sun, Q., Werne, J. P., Yang, H., Jia, J., Wang, L., Xie, H., and Chen, F.: Soil pH Dominates the Distributions of Both 5- and 6-Methyl Branched Tetraethers in Arid Regions, Journal of Geophysical Research: Biogeosciences, 125, e2019JG005 356, https://doi.org/10.1029/2019jg005356, 2020
ACA	Duan et al. (2021)	48	Northern Iran	Duan, Y.: Northern Iran and Global Soil brGDGT Dataset, https://doi.org/10.11888/Paleoenv.tpdc.271742, 2021
ACA	Guo et al. (2021)	32	China, Inner Mong.	Guo, J., Ma, T., Liu, N., Zhang, X., Hu, H., Ma, W., Wang, Z., Feng, X., and Peterse, F.: Branched Tetraether Lipids and Bacterial Communities along an Aridity Soil Transect in Inner Mongolia, Northern China, https://doi.org/10.1594/PANGAEA.938067, 2021
ACA	Kou et al. (2022)	129	China, Tibet	Kou, Q., Zhu, L., Ju, J., Wang, J., Xu, T., Li, C., and Ma, Q.: Influence of Salinity on Glycerol Dialkyl Glycerol Tetraether-Based Indicators in Tibetan Plateau Lakes: Implications for Paleotemperature and Paleosalinity Reconstructions, Palaeogeography, Palaeoclimatology, Palaeoecology, 601, 111 127, https://doi.org/10.1016/j.palaeo.2022.111127, 2022

ACA	Li et al. (2017)	11	China, Inner Mong.	Li, J., Naafs, B. D. A., Pancost, R. D., Yang, H., Liu, D., and Xie, S.: Distribution of Branched Tetraether Lipids in Ponds from Inner Mongolia, NE China: Insight into the Source of brGDGTs, Organic Geochemistry, 112, 127–136, https://doi.org/10.1016/j.orggeochem.2017.07.005, 2017
ACA	Naafs et al. (2017a)	48	Global soils	Naafs, B., Gallego-Sala, A., Inglis, G., and Pancost, R.: Refining the Global Branched Glycerol Dialkyl Glycerol Tetraether (brGDGT) Soil Temperature Calibration, Organic Geochemistry, 106, 48–56, https://doi.org/10/gbjssd, 2017
ACA	Wang et Liu (2021)	16	China	Wang, H. and Liu, W.: Soil Temperature and brGDGTs along an Elevation Gradient on the Northeastern Tibetan Plateau: A Test of Soil brGDGTs as a Proxy for Paleoelevation, Chemical Geology, 566, 120 079, https://doi.org/10.1016/j.chemgeo.2021.120079, 2021
ACA	Wang et al. (2020)	75	China	Wang, H., An, Z., Lu, H., Zhao, Z., and Liu, W.: Calibrating Bacterial Tetraether Distributions towards in Situ Soil Temperature and Application to a Loess-Paleosol Sequence, Quaternary Science Reviews, 231, 106 172, https://doi.org/10.1016/j.quascirev.2020.106172, 2020
ACA	Wang et al. (2021)	52	ACA lakes	Wang, H., Liu, W., He, Y., Zhou, A., Zhao, H., Liu, H., Cao, Y., Hu, J., Meng, B., Jiang, J., Kolpakova, M., Krivonogov, S., and Liu, Z.: Salinity-Controlled Isomerization of Lacustrine brGDGTs Impacts the Associated MBT5ME' Terrestrial Temperature Index, Geochimica et Cosmochimica Acta, 305, 33–48, https://doi.org/10.1016/j.gca.2021.05.004, 2021
ACA	Zang et al. (2018)	19	China	Zang, J., Lei, Y., and Yang, H.: Distribution of Glycerol Ethers in Turpan Soils: Implications for Use of GDGT-based Proxies in Hot and Dry Regions, Frontiers of Earth Science, 12, 862–876, https://doi.org/10/gfb6xq, 2018
WDB	Cao et al. (2020)	14	China	Cao, J., Rao, Z., Shi, F., and Jia, G.: Ice Formation on Lake Surfaces in Winter Causes Warm-Season Bias of Lacustrine brGDGT Temperature Estimates, Biogeosciences, 17, 2521–2536, https://doi.org/10.5194/bg-17-2521-2020, 2020
WDB	Dang et al. (2018)	30	China	Dang, X., Ding, W., Yang, H., Pancost, R. D., Naafs, B. D. A., Xue, J., Lin, X., Lu, J., and Xie, S.: Different Temperature Dependence of the Bacterial brGDGT Isomers in 35 Chinese Lake Sediments Compared to That in Soils, Organic Geochemistry, 119, 72–79, https://doi.org/10/gdfs3x, 2018
WDB	De Jonge et al. (2015a), Khodzher et al. (2017)	2	Russia, Baikal	De Jonge, C., Stadnitskaia, A., Fedotov, A., and Sinninghe Damsté, J. S.: Impact of Riverine Suspended Particulate Matter on the Branched Glycerol Dialkyl Glycerol Tetraether Composition of Lakes: The Outflow of the Selenga River in Lake Baikal (Russia), Organic Geochemistry, 83–84, 241–252, https://doi.org/10.1016/j.orggeochem.2015.04.004, 2015, Khodzher, T. V., Domysheva, V. M., Sorokovikova, L. M., Sakirko, M. V., and Tomberg, I. V.: Current Chemical Composition of Lake Baikal Water, Inland Waters, 7, 250–258, https://doi.org/10.1080/20442041.2017.1329982, 2017
WDB	De Jonge et al. (2019)	30	Iceland ForHot	De Jonge, C., Radujković, D., Sigurdsson, B. D., Weedon, J. T., Janssens, I., and Peterse, F.: Lipid Biomarker Temperature Proxy Responds to Abrupt Shift in the Bacterial Community Composition in Geothermally Heated Soils, Organic Geochemistry, 137, 103 897, https://doi.org/10.1016/j.orggeochem.2019.07.006, 2019
WDB	De Jonge et al. (2021)	25	Netherlands	De Jonge, C., Kuramae, E. E., Radujković, D., Weedon, J. T., Janssens, I. A., and Peterse, F.: The Influence of Soil Chemistry on Branched Tetraether Lipids in Mid-and High Latitude Soils: Implications for brGDGT-based Paleothermometry, Geochimica et Cosmochimica Acta, 310, 95–112, https://doi.org/10.1016/j.gca.2021.06.037, 2021
WDB	De Jonge et al. (2021)	25	Scotland	De Jonge, C., Kuramae, E. E., Radujković, D., Weedon, J. T., Janssens, I. A., and Peterse, F.: The Influence of Soil Chemistry on Branched Tetraether Lipids in Mid-and High Latitude Soils: Implications for brGDGT-based Paleothermometry, Geochimica et Cosmochimica Acta, 310, 95–112, https://doi.org/10.1016/j.gca.2021.06.037, 2021
WDB	Dearing Crampton-Flood et al. (2020)	61	Global BayMBT Soils	Dearing Crampton-Flood, E., Tierney, J. E., Peterse, F., Kirkels, F. M. S. A., and Sinninghe Damsté, J. S.: BayMBT: A Bayesian Calibration Model for Branched Glycerol Dialkyl Glycerol Tetraethers in Soils and Peats, Geochimica et Cosmochimica Acta, 268, 142–159, https://doi.org/10/gg9758, 2020
WDB	Ding et al. (2018)	22	Germany	Ding, S., Kohlhepp, B., Trumbore, S., Küsel, K., Totsche, K.-U., Pohnert, G., Gleixner, G., and Schwab, V. F.: In Situ Production of Core and Intact Bacterial and Archaeal Tetraether Lipids in Groundwater, Organic Geochemistry, 126, 1–12, https://doi.org/10.1016/j.orggeochem.2018.10.005, 2018
WDB	Guo et al. (2020)	74	England	Guo, J., Glendell, M., Meersmans, J., Kirkels, F., Middelburg, J. J., and Peterse, F.: Assessing Branched Tetraether Lipids as Tracers of Soil Organic Carbon Transport through the Carminowe Creek Catchment (Southwest England), Biogeosciences, 17, 3183–3201, https://doi.org/10.5194/bg-17-3183-2020, 2020

WDB	Kirkels et al. (2019)	28	Amazon
WDB	Kusch et al. (2019)	17	Siberia
WDB	Li et al. (2018)	29	China
WDB	Martínez-Sosa et al. (2019)	20	USA
WDB	Martínez-Sosa et al. (2020)	16	USA
WDB	Martínez-Sosa et al. (2021)	158	Global
WDB	Miller et al. (2018)	30	USA
WDB	Naafs et al. (2017a)	302	Global soils
WDB	Ning et al. (2019)	2	China
WDB	Pei et al. (2019)	10	China
WDB	Pérez-Angel et al. (2020)	36	Colombia
WDB	Qian et al. (2019)	17	China
WDB	Raberg et al. (2021)	43	Baffin
WDB	Raberg et al. (2021)	43	Iceland
WDB	Russell et al. (2018)	65	Africa

Kirkels, F. M. S. A., Ponton, C., Galy, V., West, A. J., Feakins, S. J., and Peterse, F.: From Andes to Amazon: Assessing Branched Tetraether Lipids as Tracers for Soil Organic Carbon in the Madre de Dios River System, Journal of Geophysical Research: Biogeosciences, 125, e2019JG005 270, https://doi.org/10.1029/2019JG005270, 2020

Kusch, S., Winterfeld, M., Mollenhauer, G., Höfle, S. T., Schirrmeister, L., Schwamborn, G., and Rethemeyer, J.: Glycerol Dialkyl Glycerol Tetraethers (GDGTs) in High Latitude Siberian Permafrost: Diversity, Environmental Controls, and Implications for Proxy Applications, Organic Geochemistry, 136, 103 888, https://doi.org/10.1016/j.orggeochem.2019.06.009, 2019

Li, Y., Zhao, S., Pei, H., Qian, S., Zang, J., Dang, X., and Yang, H.: Distribution of Glycerol Dialkyl Glycerol Tetraethers in Surface Soils along an Altitudinal Transect at Cold and Humid Mountain Changbai: Implications for the Reconstruction of Paleoaltimetry and Paleoclimate, Science China Earth Sciences, 61, 925–939, https://doi.org/10.1007/s11430-017-9168-9, 2018

Martínez-Sosa, P. and Tierney, J. E.: Lacustrine brGDGT Response to Microcosm and Mesocosm Incubations, Organic Geochemistry, 127, 12–22, https://doi.org/10.1016/j.orggeochem.2018.10.011, 2019

Martínez-Sosa, P., Tierney, J. E., and Meredith, L. K.: Controlled Lacustrine Microcosms Show a brGDGT Response to Environmental Perturbations, Organic Geochemistry, 145, 104 041, https://doi.org/10/ggvt59, 2020

Martínez-Sosa, P., Tierney, J. E., Stefanescu, I. C., Crampton-Flood, E. D., Shuman, B. N., and Routson, C.: A Global Bayesian Temperature Calibration for Lacustrine brGDGTs, Geochimica et Cosmochimica Acta, 305, 87–105, https://doi.org/10.1016/j.gca.2021.04.038, 2021

Miller, D. R., Habicht, M. H., Keisling, B. A., Castañeda, I. S., and Bradley, R. S.: A 900-Year New England Temperature Reconstruction from in Situ Seasonally Produced Branched Glycerol Dialkyl Glycerol Tetraethers (brGDGTs), Climate of the Past, 14, 1653–1667, https://doi.org/10.5194/cp-14-1653-2018, 2018

Naafs, B., Gallego-Sala, A., Inglis, G., and Pancost, R.: Refining the Global Branched Glycerol Dialkyl Glycerol Tetraether (brGDGT) Soil Temperature Calibration, Organic Geochemistry, 106, 48–56, https://doi.org/10/gbjssd, 2017

Ning, D., Zhang, E., Shulmeister, J., Chang, J., Sun, W., and Ni, Z.: Holocene Mean Annual Air Temperature (MAAT) Reconstruction Based on Branched Glycerol Dialkyl Glycerol Tetraethers from Lake Ximenglongtan, Southwestern China, Organic Geochemistry, https://doi.org/10.1016/j.orggeochem.2019.05.003, 2019

Pei, H., Wang, C., Wang, Y., Yang, H., and Xie, S.: Distribution of Microbial Lipids at an Acid Mine Drainage Site in China: Insights into Microbial Adaptation to Extremely Low pH Conditions, Organic Geochemistry, 134, 77–91, https://doi.org/10.1016/j.orggeochem.2019.05.008, 2019

Pérez-Angel, L. C., Sepúlveda, J., Molnar, P., Montes, C., Rajagopalan, B., Snell, K., Gonzalez-Arango, C., and Dildar, N.: Soil and Air Temperature Calibrations Using Branched GDGTs for the Tropical Andes of Colombia: Toward a Pan-Tropical Calibration, Geochemistry, Geophysics, Geosystems, 21, e2020GC008 941, https://doi.org/10.1029/2020GC008941, 2020

Qian, S., Yang, H., Dong, C., Wang, Y., Wu, J., Pei, H., Dang, X., Lu, J., Zhao, S., and Xie, S.: Rapid Response of Fossil Tetraether Lipids in Lake Sediments to Seasonal Environmental Variables in a Shallow Lake in Central China: Implications for the Use of Tetraether-Based Proxies, Organic Geochemistry, 128, 108–121, https://doi.org/10.1016/j.orggeochem.2018.12.007, 2019

Raberg, J. H., Harning, D. J., Crump, S. E., de Wet, G., Blumm, A., Kopf, S., Geirsdóttir, Á., Miller, G. H., and Sepúlveda, J.: Revised Fractional Abundances and Warm-Season Temperatures Substantially Improve brGDGT Calibrations in Lake Sediments, Biogeosciences, 18, 3579–3603, https://doi.org/10.5194/bg-18-3579-2021, 2021

Raberg, J. H., Harning, D. J., Crump, S. E., de Wet, G., Blumm, A., Kopf, S., Geirsdóttir, Á., Miller, G. H., and Sepúlveda, J.: Revised Fractional Abundances and Warm-Season Temperatures Substantially Improve brGDGT Calibrations in Lake Sediments, Biogeosciences, 18, 3579–3603, https://doi.org/10.5194/bg-18-3579-2021, 2021

Russell, J. M., Hopmans, E. C., Loomis, S. E., Liang, J., and Damsté, J. S. S.: Distributions of 5-and 6-Methyl Branched Glycerol Dialkyl Glycerol Tetraethers (brGDGTs) in East African Lake Sediment: Effects of Temperature, pH, and New Lacustrine Paleotemperature Calibrations, Organic Geochemistry, 117, 56–69, https://doi.org/10.1016/j.orggeochem.2017.12.003, 2018

WDB	Véquaud et al. (2021)	49	France	Véquaud, P., Derenne, S., Anquetil, C., Collin, S., Poulenard, J., Sabatier, P., and Huguet, A.: Influence of Environmental Parameters on the Distribution of Bacterial Lipids in Soils from the French Alps: Implications for Paleo-Reconstructions, Organic Geochemistry, p. 104194, https://doi.org/10.1016/j.orggeochem.2021.104194, 2021
WDB	Wang et al. (2018)	28	China	Wang, M., Zong, Y., Zheng, Z., Man, M., Hu, J., and Tian, L.: Utility of brGDGTs as Temperature and Precipitation Proxies in Subtropical China, Scientific Reports, 8, 1–9, https://doi.org/10.1038/s41598-017-17964-0, 2018
WDB	Wang et al. (2019)	47	China	Wang, M., Zheng, Z., Zong, Y., Man, M., and Tian, L.: Distributions of Soil Branched Glycerol Dialkyl Glycerol Tetraethers from Different Climate Regions of China, Scientific reports, 9, 1–8, https://doi.org/10.1038/s41598-019-39147-9, 2019
WDB	Wang et al. (2020)	74	China	Wang, H., An, Z., Lu, H., Zhao, Z., and Liu, W.: Calibrating Bacterial Tetraether Distributions towards in Situ Soil Temperature and Application to a Loess-Paleosol Sequence, Quaternary Science Reviews, 231, 106 172, https://doi.org/10.1016/j.quascirev.2020.106172, 2020
WDB	Weber et al. (2018)	133	Switzerland	Weber, Y., Damsté, J. S. S., Zopfi, J., De Jonge, C., Gilli, A., Schubert, C. J., Lepori, F., Lehmann, M. F., and Niemann, H.: Redox-Dependent Niche Differentiation Provides Evidence for Multiple Bacterial Sources of Glycerol Tetraether Lipids in Lakes, Proceedings of the National Academy of Sciences, 115, 10 926–10 931, https://doi.org/10.1073/pnas.1805186115, 2018
WDB	Wu et al. (2021)	4	China	Wu, J., Yang, H., Pancost, R. D., Naafs, B. D. A., Qian, S., Dang, X., Sun, H., Pei, H., Wang, R., Zhao, S., and Xie, S.: Variations in Dissolved O2 in a Chinese Lake Drive Changes in Microbial Communities and Impact Sedimentary GDGT Distributions, Chemical Geology, 579, 120 348, https://doi.org/10.1016/j.chemgeo.2021.120348, 2021
WDB	Yao et al. (2019), Yao et al. (2020), Woltering et al. (2012)	32	China	Yao, Y., Zhao, J., Bauersachs, T., and Huang, Y.: Effect of Water Depth on the TEX86 Proxy in Volcanic Lakes of Northeastern China, Organic Geochemistry, 129, 88–98, https://doi.org/10.1016/j.orggeochem.2019.01.014, 2019, Yao, Y., Zhao, J., Vachula, R. S., Werne, J. P., Wu, J., Song, X., and Huang, Y.: Correlation between the Ratio of 5-Methyl Hexamethylated to Pentamethylated Branched GDGTs (HP5) and Water Depth Reflects Redox Variations in Stratified Lakes, Organic Geochemistry, 147, 104 076, https://doi.org/10.1016/j.orggeochem.2020.104076, 2020, Woltering, M., Werne, J. P., Kish, J. L., Hicks, R., Damsté, J. S. S., and Schouten, S.: Vertical and Temporal Variability in Concentration and Distribution of Thaumarchaeotal Tetraether Lipids in Lake Superior and the Implications for the Application of the TEX86 Temperature Proxy, Geochimica et Cosmochimica Acta, 87, 136–153, https://doi.org/10.1016/j.gca.2012.03.024, 2012
WDB	Yao et al. (2019), Yao et al. (2020), Woltering et al. (2012)	32	USA	Yao, Y., Zhao, J., Bauersachs, T., and Huang, Y.: Effect of Water Depth on the TEX86 Proxy in Volcanic Lakes of Northeastern China, Organic Geochemistry, 129, 88–98, https://doi.org/10.1016/j.orggeochem.2019.01.014, 2019, Yao, Y., Zhao, J., Vachula, R. S., Werne, J. P., Wu, J., Song, X., and Huang, Y.: Correlation between the Ratio of 5-Methyl Hexamethylated to Pentamethylated Branched GDGTs (HP5) and Water Depth Reflects Redox Variations in Stratified Lakes, Organic Geochemistry, 147, 104 076, https://doi.org/10.1016/j.orggeochem.2020.104076, 2020, Woltering, M., Werne, J. P., Kish, J. L., Hicks, R., Damsté, J. S. S., and Schouten, S.: Vertical and Temporal Variability in Concentration and Distribution of Thaumarchaeotal Tetraether Lipids in Lake Superior and the Implications for the Application of the TEX86 Temperature Proxy, Geochimica et Cosmochimica Acta, 87, 136–153, https://doi.org/10.1016/j.gca.2012.03.024, 2012
WDB	Zhao et al. (2021)	9	Greenland	Zhao, B., Castañeda, I. S., Bradley, R. S., Salacup, J. M., de Wet, G. A., Daniels, W. C., and Schneider, T.: Development of an in Situ Branched GDGT Calibration in Lake 578, Southern Greenland, Organic Geochemistry, 152, 104 168, https://doi.org/10.1016/j.orggeochem.2020.104168, 2021
WDB	van Bree et al. (2020)	196	Africa	van Bree, L. G., Peterse, F., Baxter, A. J., De Crop, W., Van Grinsven, S., Villanueva, L., Verschuren, D., and Sinninghe Damsté, J. S.: Seasonal Variability and Sources of in Situ brGDGT Production in a Permanently Stratified African Crater Lake, Biogeosciences Discussions, 2020, 1–36, 2020

Table S.3. Presentation of the different thresholds associated with each of the grouping factor used in this study.

	ID	Classes	Threshold
Alkalinity	1	Acid	pH < 7
	2	Neutral	$\mathrm{pH} \in [7;8[$
	3	Alkaline	$\mathrm{pH} \geq 8$
Aridity	1	Hyper-arid	AI < 1500
	2	Arid	$\mathrm{AI} \in [1500;3000[$
	3	Semi-arid	$\mathrm{AI} \in [3000;3700[$
	4	Dry sub-humid	$\mathrm{AI} \in [3700;5500[$
	5	Humid	$\mathrm{AI} \geq 5500$
Salinity	1	Fresh	Salinity < 700
	2	Hyposaline	$\mathrm{Salinity} \in [700;26000[$
	3	Saline	$\mathrm{Salinity} \in [26;140000[$
	4	Hypersaline	$\mathrm{Salinity} \geq 140000$
Sample type	1	Soil	
	2	Lacustrine	

Table S.4. Results of the Variance Factors analyses (VIF) carried out on the brGDGT FAs vs. climate parameter for model 1 (i.e., all the available climate parameters) and model 2 (after removing the covariant climate parameters owing to only having VIFs < 10).

Climate parameters	VIF (model 1)	VIF (model 2)
AI	21.60	3.00
Altitude	22.20	
MAAT	620.60	5.60
MAF	28.00	4.40
MAP	37.80	
MPCOQ	17.80	
MPWAQ	16.70	3.20
MTCOQ	159.10	
MTWAQ	271.60	
pH	1.70	1.70
Salinity	1.30	1.30

Table S.5. Levene's test results for the two MANOVA models used to evaluate the grouping factors effect across brGDGT FA and indices. The violation of the assumption of homogeneity of variance-covariance is marked by ** (p-values < 0.001) or * (p-values < 0.01)

	Alkalinity	**Aridity**	**Salinity**	**Sample type**
f(IIIa)			**	
f(IIIa')			**	*
f(IIIb)			*	
f(IIIb')				
f(IIIc)				**
f(IIIc')				*
f(IIa)		**	**	
f(IIa')				
f(IIb)				
f(IIb')			**	
f(IIc)				
f(IIc')				
f(Ia)	*	**		
f(Ib)				
f(Ic)				*
MBT'_{5Me}		**	*	
MBT'_{6Me}	**	*		
IR_{6Me}				
IR_{6+7Me}	*			
IR'_{6+7Me}	*		**	
CBT'		*		
CBT'_{5Me}		**		*

References

Cao, J., Rao, Z., Shi, F., and Jia, G.: Ice Formation on Lake Surfaces in Winter Causes Warm-Season Bias of Lacustrine brGDGT Temperature Estimates, Biogeosciences, 17, 2521–2536, https://doi.org/10.5194/bg-17-2521-2020, 2020.

Chen, C., Bai, Y., Fang, X., Zhuang, G., Khodzhiev, A., Bai, X., and Murodov, A.: Evaluating the Potential of Soil Bacterial Tetraether Proxies in Westerlies Dominating Western Pamirs, Tajikistan and Implications for Paleoenvironmental Reconstructions, Chemical Geology, 559, 119 908, https://doi.org/10.1016/j.chemgeo.2020.119908, 2021.

Clogg, C. C., Petkova, E., and Haritou, A.: Statistical Methods for Comparing Regression Coefficients between Models, American Journal Of Sociology, 100, 1261–1293, https://doi.org/10.1086/230638, 1995.

Dang, X., Ding, W., Yang, H., Pancost, R. D., Naafs, B. D. A., Xue, J., Lin, X., Lu, J., and Xie, S.: Different Temperature Dependence of the Bacterial brGDGT Isomers in 35 Chinese Lake Sediments Compared to That in Soils, Organic Geochemistry, 119, 72–79, https://doi.org/10/gdfs3x, 2018.

De Jonge, C., Stadnitskaia, A., Fedotov, A., and Sinninghe Damsté, J. S.: Impact of Riverine Suspended Particulate Matter on the Branched Glycerol Dialkyl Glycerol Tetraether Composition of Lakes: The Outflow of the Selenga River in Lake Baikal (Russia), Organic Geochemistry, 83–84, 241–252, https://doi.org/10.1016/j.orggeochem.2015.04.004, 2015.

De Jonge, C., Radujković, D., Sigurdsson, B. D., Weedon, J. T., Janssens, I., and Peterse, F.: Lipid Biomarker Temperature Proxy Responds to Abrupt Shift in the Bacterial Community Composition in Geothermally Heated Soils, Organic Geochemistry, 137, 103 897, https://doi.org/10.1016/j.orggeochem.2019.07.006, 2019.

De Jonge, C., Kuramae, E. E., Radujković, D., Weedon, J. T., Janssens, I. A., and Peterse, F.: The Influence of Soil Chemistry on Branched Tetraether Lipids in Mid-and High Latitude Soils: Implications for brGDGT-based Paleothermometry, Geochimica et Cosmochimica Acta, 310, 95–112, https://doi.org/10.1016/j.gca.2021.06.037, 2021.

Dearing Crampton-Flood, E., Tierney, J. E., Peterse, F., Kirkels, F. M. S. A., and Sinninghe Damsté, J. S.: BayMBT: A Bayesian Calibration Model for Branched Glycerol Dialkyl Glycerol Tetraethers in Soils and Peats, Geochimica et Cosmochimica Acta, 268, 142–159, https://doi.org/10/gg9758, 2020.

Ding, S., Kohlhepp, B., Trumbore, S., Küsel, K., Totsche, K.-U., Pohnert, G., Gleixner, G., and Schwab, V. F.: In Situ Production of Core and Intact Bacterial and Archaeal Tetraether Lipids in Groundwater, Organic Geochemistry, 126, 1–12, https://doi.org/10.1016/j.orggeochem.2018.10.005, 2018.

Duan, Y.: Northern Iran and Global Soil brGDGT Dataset, https://doi.org/10.11888/Paleoenv.tpdc.271742, 2021.

Duan, Y., Sun, Q., Werne, J. P., Yang, H., Jia, J., Wang, L., Xie, H., and Chen, F.: Soil pH Dominates the Distributions of Both 5- and 6-Methyl Branched Tetraethers in Arid Regions, Journal of Geophysical Research: Biogeosciences, 125, e2019JG005 356, https://doi.org/10.1029/2019jg005356, 2020.

Fick, S. E. and Hijmans, R. J.: WorldClim 2: New 1-Km Spatial Resolution Climate Surfaces for Global Land Areas: NEW CLIMATE SURFACES FOR GLOBAL LAND AREAS, International Journal of Climatology, 37, 4302–4315, https://doi.org/10/gb2jnq, 2017.

Guo, J., Glendell, M., Meersmans, J., Kirkels, F., Middelburg, J. J., and Peterse, F.: Assessing Branched Tetraether Lipids as Tracers of Soil Organic Carbon Transport through the Carminowe Creek Catchment (Southwest England), Biogeosciences, 17, 3183–3201, https://doi.org/10.5194/bg-17-3183-2020, 2020.

Guo, J., Ma, T., Liu, N., Zhang, X., Hu, H., Ma, W., Wang, Z., Feng, X., and Peterse, F.: Branched Tetraether Lipids and Bacterial Communities along an Aridity Soil Transect in Inner Mongolia, Northern China, https://doi.org/10.1594/PANGAEA.938067, 2021.

Khodzher, T. V., Domysheva, V. M., Sorokovikova, L. M., Sakirko, M. V., and Tomberg, I. V.: Current Chemical Composition of Lake Baikal Water, Inland Waters, 7, 250–258, https://doi.org/10.1080/20442041.2017.1329982, 2017.

Kirkels, F. M. S. A., Ponton, C., Galy, V., West, A. J., Feakins, S. J., and Peterse, F.: From Andes to Amazon: Assessing Branched Tetraether Lipids as Tracers for Soil Organic Carbon in the Madre de Dios River System, Journal of Geophysical Research: Biogeosciences, 125, e2019JG005 270, https://doi.org/10.1029/2019JG005270, 2020.

Kou, Q., Zhu, L., Ju, J., Wang, J., Xu, T., Li, C., and Ma, Q.: Influence of Salinity on Glycerol Dialkyl Glycerol Tetraether-Based Indicators in Tibetan Plateau Lakes: Implications for Paleotemperature and Paleosalinity Reconstructions, Palaeogeography, Palaeoclimatology, Palaeoecology, 601, 111 127, https://doi.org/10.1016/j.palaeo.2022.111127, 2022.

Kusch, S., Winterfeld, M., Mollenhauer, G., Höfle, S. T., Schirrmeister, L., Schwamborn, G., and Rethemeyer, J.: Glycerol Dialkyl Glycerol Tetraethers (GDGTs) in High Latitude Siberian Permafrost: Diversity, Environmental Controls, and Implications for Proxy Applications, Organic Geochemistry, 136, 103 888, https://doi.org/10.1016/j.orggeochem.2019.06.009, 2019.

Li, J., Naafs, B. D. A., Pancost, R. D., Yang, H., Liu, D., and Xie, S.: Distribution of Branched Tetraether Lipids in Ponds from Inner Mongolia, NE China: Insight into the Source of brGDGTs, Organic Geochemistry, 112, 127–136, https://doi.org/10.1016/j.orggeochem.2017.07.005, 2017.

Li, Y., Zhao, S., Pei, H., Qian, S., Zang, J., Dang, X., and Yang, H.: Distribution of Glycerol Dialkyl Glycerol Tetraethers in Surface Soils along an Altitudinal Transect at Cold and Humid Mountain Changbai: Implications for the Reconstruction of Paleoaltimetry and Paleoclimate, Science China Earth Sciences, 61, 925–939, https://doi.org/10.1007/s11430-017-9168-9, 2018.

Martínez-Sosa, P. and Tierney, J. E.: Lacustrine brGDGT Response to Microcosm and Mesocosm Incubations, Organic Geochemistry, 127, 12–22, https://doi.org/10.1016/j.orggeochem.2018.10.011, 2019.

Martínez-Sosa, P., Tierney, J. E., and Meredith, L. K.: Controlled Lacustrine Microcosms Show a brGDGT Response to Environmental Perturbations, Organic Geochemistry, 145, 104 041, https://doi.org/10/ggvt59, 2020.

Martínez-Sosa, P., Tierney, J. E., Stefanescu, I. C., Crampton-Flood, E. D., Shuman, B. N., and Routson, C.: A Global Bayesian Temperature Calibration for Lacustrine brGDGTs, Geochimica et Cosmochimica Acta, 305, 87–105, https://doi.org/10.1016/j.gca.2021.04.038, 2021.

Miller, D. R., Habicht, M. H., Keisling, B. A., Castañeda, I. S., and Bradley, R. S.: A 900-Year New England Temperature Reconstruction from in Situ Seasonally Produced Branched Glycerol Dialkyl Glycerol Tetraethers (brGDGTs), Climate of the Past, 14, 1653–1667, https://doi.org/10.5194/cp-14-1653-2018, 2018.

Naafs, B., Gallego-Sala, A., Inglis, G., and Pancost, R.: Refining the Global Branched Glycerol Dialkyl Glycerol Tetraether (brGDGT) Soil Temperature Calibration, Organic Geochemistry, 106, 48–56, https://doi.org/10/gbjssd, 2017.

Ning, D., Zhang, E., Shulmeister, J., Chang, J., Sun, W., and Ni, Z.: Holocene Mean Annual Air Temperature (MAAT) Reconstruction Based on Branched Glycerol Dialkyl Glycerol Tetraethers from Lake Ximenglongtan, Southwestern China, Organic Geochemistry, https://doi.org/10.1016/j.orggeochem.2019.05.003, 2019.

Pei, H., Wang, C., Wang, Y., Yang, H., and Xie, S.: Distribution of Microbial Lipids at an Acid Mine Drainage Site in China: Insights into Microbial Adaptation to Extremely Low pH Conditions, Organic Geochemistry, 134, 77–91, https://doi.org/10.1016/j.orggeochem.2019.05.008, 2019.

Pérez-Angel, L. C., Sepúlveda, J., Molnar, P., Montes, C., Rajagopalan, B., Snell, K., Gonzalez-Arango, C., and Dildar, N.: Soil and Air Temperature Calibrations Using Branched GDGTs for the Tropical Andes of Colombia: Toward a Pan-Tropical Calibration, Geochemistry, Geophysics, Geosystems, 21, e2020GC008 941, https://doi.org/10.1029/2020GC008941, 2020.

Qian, S., Yang, H., Dong, C., Wang, Y., Wu, J., Pei, H., Dang, X., Lu, J., Zhao, S., and Xie, S.: Rapid Response of Fossil Tetraether Lipids in Lake Sediments to Seasonal Environmental Variables in a Shallow Lake in Central China: Implications for the Use of Tetraether-Based Proxies, Organic Geochemistry, 128, 108–121, https://doi.org/10.1016/j.orggeochem.2018.12.007, 2019.

Raberg, J. H., Harning, D. J., Crump, S. E., de Wet, G., Blumm, A., Kopf, S., Geirsdóttir, Á., Miller, G. H., and Sepúlveda, J.: Revised Fractional Abundances and Warm-Season Temperatures Substantially Improve brGDGT Calibrations in Lake Sediments, Biogeosciences, 18, 3579–3603, https://doi.org/10.5194/bg-18-3579-2021, 2021.

Raberg, J. H., Flores, E., Crump, S. E., de Wet, G., Dildar, N., Miller, G. H., Geirsdóttir, Á., and Sepúlveda, J.: Intact Polar brGDGTs in Arctic Lake Catchments: Implications for Lipid Sources and Paleoclimate Applications, Journal of Geophysical Research: Biogeosciences, 127, e2022JG006 969, https://doi.org/10.1029/2022JG006969, 2022.

Russell, J. M., Hopmans, E. C., Loomis, S. E., Liang, J., and Damsté, J. S. S.: Distributions of 5-and 6-Methyl Branched Glycerol Dialkyl Glycerol Tetraethers (brGDGTs) in East African Lake Sediment: Effects of Temperature, pH, and New Lacustrine Paleotemperature Calibrations, Organic Geochemistry, 117, 56–69, https://doi.org/10.1016/j.orggeochem.2017.12.003, 2018.

van Bree, L. G., Peterse, F., Baxter, A. J., De Crop, W., Van Grinsven, S., Villanueva, L., Verschuren, D., and Sinninghe Damsté, J. S.: Seasonal Variability and Sources of in Situ brGDGT Production in a Permanently Stratified African Crater Lake, Biogeosciences Discussions, 2020, 1–36, 2020.

Véquaud, P., Derenne, S., Anquetil, C., Collin, S., Poulenard, J., Sabatier, P., and Huguet, A.: Influence of Environmental Parameters on the Distribution of Bacterial Lipids in Soils from the French Alps: Implications for Paleo-Reconstructions, Organic Geochemistry, p. 104194, https://doi.org/10.1016/j.orggeochem.2021.104194, 2021.

Wang, H. and Liu, W.: Soil Temperature and brGDGTs along an Elevation Gradient on the Northeastern Tibetan Plateau: A Test of Soil brGDGTs as a Proxy for Paleoelevation, Chemical Geology, 566, 120 079, https://doi.org/10.1016/j.chemgeo.2021.120079, 2021.

Wang, H., An, Z., Lu, H., Zhao, Z., and Liu, W.: Calibrating Bacterial Tetraether Distributions towards in Situ Soil Temperature and Application to a Loess-Paleosol Sequence, Quaternary Science Reviews, 231, 106 172, https://doi.org/10.1016/j.quascirev.2020.106172, 2020.

Wang, H., Liu, W., He, Y., Zhou, A., Zhao, H., Liu, H., Cao, Y., Hu, J., Meng, B., Jiang, J., Kolpakova, M., Krivonogov, S., and Liu, Z.: Salinity-Controlled Isomerization of Lacustrine brGDGTs Impacts the Associated MBT5ME' Terrestrial Temperature Index, Geochimica et Cosmochimica Acta, 305, 33–48, https://doi.org/10.1016/j.gca.2021.05.004, 2021.

Wang, M., Zong, Y., Zheng, Z., Man, M., Hu, J., and Tian, L.: Utility of brGDGTs as Temperature and Precipitation Proxies in Subtropical China, Scientific Reports, 8, 1–9, https://doi.org/10.1038/s41598-017-17964-0, 2018.

Wang, M., Zheng, Z., Zong, Y., Man, M., and Tian, L.: Distributions of Soil Branched Glycerol Dialkyl Glycerol Tetraethers from Different Climate Regions of China, Scientific reports, 9, 1–8, https://doi.org/10.1038/s41598-019-39147-9, 2019.

Weber, Y., Damsté, J. S. S., Zopfi, J., De Jonge, C., Gilli, A., Schubert, C. J., Lepori, F., Lehmann, M. F., and Niemann, H.: Redox-Dependent Niche Differentiation Provides Evidence for Multiple Bacterial Sources of Glycerol Tetraether Lipids in Lakes, Proceedings of the National Academy of Sciences, 115, 10 926–10 931, https://doi.org/10.1073/pnas.1805186115, 2018.

Woltering, M., Werne, J. P., Kish, J. L., Hicks, R., Damsté, J. S. S., and Schouten, S.: Vertical and Temporal Variability in Concentration and Distribution of Thaumarchaeotal Tetraether Lipids in Lake Superior and the Implications for the Application of the TEX86 Temperature Proxy, Geochimica et Cosmochimica Acta, 87, 136–153, https://doi.org/10.1016/j.gca.2012.03.024, 2012.

Wu, J., Yang, H., Pancost, R. D., Naafs, B. D. A., Qian, S., Dang, X., Sun, H., Pei, H., Wang, R., Zhao, S., and Xie, S.: Variations in Dissolved O2 in a Chinese Lake Drive Changes in Microbial Communities and Impact Sedimentary GDGT Distributions, Chemical Geology, 579, 120 348, https://doi.org/10.1016/j.chemgeo.2021.120348, 2021.

Yao, Y., Zhao, J., Bauersachs, T., and Huang, Y.: Effect of Water Depth on the TEX86 Proxy in Volcanic Lakes of Northeastern China, Organic Geochemistry, 129, 88–98, https://doi.org/10.1016/j.orggeochem.2019.01.014, 2019.

Yao, Y., Zhao, J., Vachula, R. S., Werne, J. P., Wu, J., Song, X., and Huang, Y.: Correlation between the Ratio of 5-Methyl Hexamethylated to Pentamethylated Branched GDGTs (HP5) and Water Depth Reflects Redox Variations in Stratified Lakes, Organic Geochemistry, 147, 104 076, https://doi.org/10.1016/j.orggeochem.2020.104076, 2020.

Zang, J., Lei, Y., and Yang, H.: Distribution of Glycerol Ethers in Turpan Soils: Implications for Use of GDGT-based Proxies in Hot and Dry Regions, Frontiers of Earth Science, 12, 862–876, https://doi.org/10/gfb6xq, 2018.

Zhao, B., Castañeda, I. S., Bradley, R. S., Salacup, J. M., de Wet, G. A., Daniels, W. C., and Schneider, T.: Development of an in Situ Branched GDGT Calibration in Lake 578, Southern Greenland, Organic Geochemistry, 152, 104 168, https://doi.org/10.1016/j.orggeochem.2020.104168, 2021.